DOI 10.1515/nanoph-2013-0013 — Nanophotonics 2014; 3(4-5): 269–281

Review article

Kishore Padmaraju* and Keren Bergman

Resolving the thermal challenges for silicon microring resonator devices

Abstract: Silicon microring resonators have been hailed for their potential use in next-generation optical interconnects. However, the functionality of silicon microring based devices suffer from susceptibility to thermal fluctuations that is often overlooked in their demonstrated results, but must be resolved for their future implementation in microelectronic applications. We survey the emerging efforts that have been put forth to resolve these thermal susceptibilities and provide a comprehensive discussion of their advantages and disadvantages.

Keywords: integrated photonics; microring resonators; optical interconnects; silicon photonics.

***Corresponding author: Kishore Padmaraju,** Department of Electrical Engineering, Columbia University, 500 West 120th Street, New York, NY, USA, e-mail: kpadmara@ee.columbia.edu
Keren Bergman: Department of Electrical Engineering, Columbia University, 500 West 120th Street, New York, NY, USA

Edited by Michal Lipson

1 Silicon microring resonator based devices

The growing bandwidth needs within data applications have motivated the replacement of traditionally electronic links with optical links for information networks as diverse as data centers, supercomputers, and fiber-optic access networks [1, 2]. Applications such as these stress the traditional portfolio of optical components, rebalancing the emphasis from expensive high-performance components towards low-cost high-volume components that can be closely integrated with electronics. With these considerations in mind, the silicon photonics platform has received wide attention for its ability to deliver the necessary bandwidth required at an economy-of-scale that will be enabled by its compatibility with CMOS fabrication processes [3].

Within the silicon photonic platform, traditional optical components such as low-loss waveguides [4], low-loss waveguide crossings [5], high-speed mach-zhender modulators (MZM) [6], arrayed waveguide-gratings [7], and efficient photodetectors [8, 9] have been demonstrated. Leveraging the high index contrast between silicon and silicon-on-insulator, the aforementioned components have been shown with much smaller footprints than their counterparts in more conventional optical platforms. For active devices, these smaller footprints directly translate to higher energy-efficiencies.

In addition to providing these improvements in footprint and energy-efficiency for traditional devices, the high-index contrast present in the silicon photonic platform enables the effective use of microring-based devices. A microring is a traveling wave resonator consisting of a ring structure side-coupled to a bus waveguide. While they have also been demonstrated in other material platforms, the high-index contrast of silicon and silicon-on-insulator has allowed them to be manifested as small as 1.5 μm in radius [10], and when used in conjunction with the free-carrier dispersion effect [11], well into Ghz-rate bandwidth. Figure 1A illustrates the optical resonance of the microring and its shift with applied electrical bias [12]. In their most basic capacity they can serve as effective filters [13], switches [14, 15], and modulators [16, 17]. Additionally, microrings can be cascaded along the same waveguide bus, with each microring being offset to provide functionality for a specific wavelength. In this manner, the microring lends itself naturally for wavelength-division-multiplexed (WDM) operation, a common solution for multiplying the bandwidth of optical links [18]. Figure 2 illustrates the cascading of microring modulators for the generation of WDM optical data; this same configuration can be used on the receive side to subsequently demultiplex a WDM stream.

Microring-based devices push the limits on footprint and energy efficiency and provide an ideal solution for enabling low-cost WDM communication within the silicon photonics platform. Commercially implemented microring-based optical networks will likely be

© 2014 Science Wise Publishing & De Gruyter

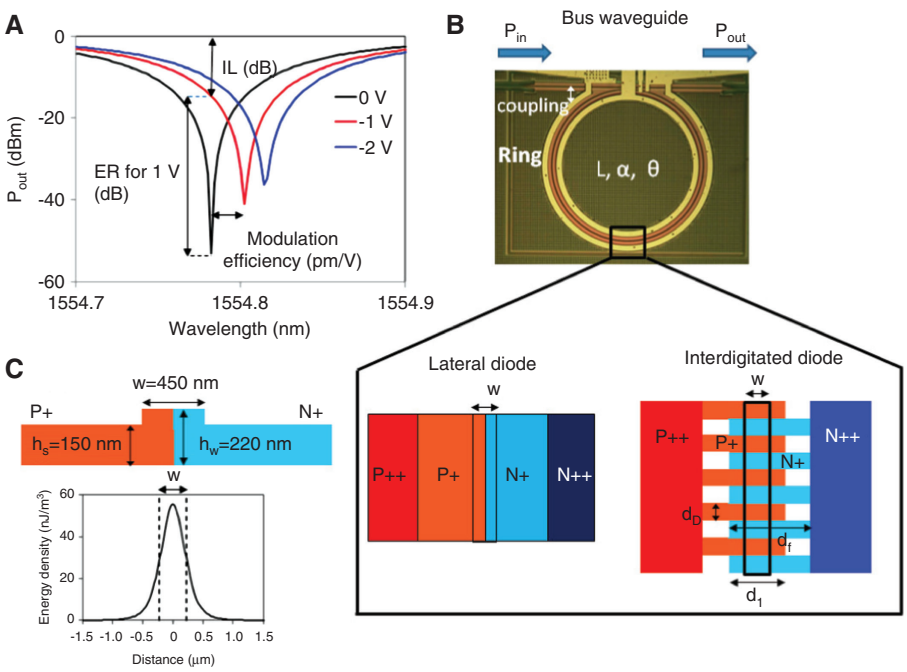

Figure 1 (A) Typical transmission spectra of carrier depletion ring modulator for different applied bias. (B) Ring modulator schematic showing a lateral and interdigitated diode design. (C) Ring waveguide cross-section and optical mode distribution. Reprinted with permission from Ref. [12], copyright (2013) IEEE.

application-tailored through the optimization of such microring characteristics as optical insertion loss, cross-talk, footprint, modulation-bandwidth, -linearity, and -depth [19–22]. However, superseding these parameters in importance is the issue of thermal susceptibility. For the successful migration of microring resonators from academic novelty to commercial implementation, the thermal challenges that plague silicon microring-based devices must be resolved.

2 Thermal effects on microring resonator based devices

Most optical devices exhibit some vulnerability to temperature changes. However, the high thermo-optic coefficient of silicon (1.86×10^{-4} K^{-1}) and the wavelength selectivity of microring resonators make them especially susceptible to fluctuations in temperature [23]. The shift in the resonant

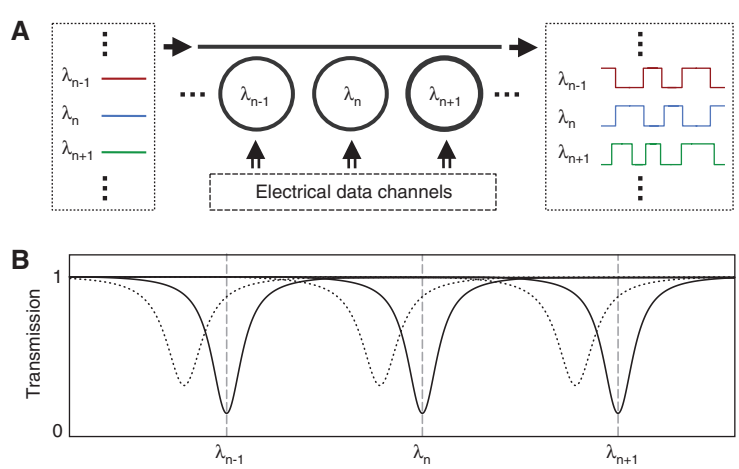

Figure 2 (A) Microring modulators of varying radii can be cascaded along a waveguide bus to generate WDM optical modulation. (B) Transmission spectrum for densely spaced WDM microring modulators.

wavelength of a microring with respect to temperature is given by

$$\frac{d\lambda}{dT}=\left(n_{eff}\alpha_{sub}+\frac{\partial n_{eff}}{\partial T}\right)\frac{\lambda_0}{n_g} \quad (1)$$

where λ_0 is the resonant wavelength, n_{eff} is the effective index, α_{sub} is the substrate expansion coefficient, and n_g is the group index [24, 25]. While not indicated in Eq. (1), these terms will have wavelength dependence. Because the optical mode is tightly confined in the silicon core, and also because the thermo-optic coefficient of SiO_2 (1×10^{-5} K^{-1}) is a magnitude lower than that of Si, the corresponding contribution is omitted from Eq. (1). Additionally, because α_{sub} (2.6×10^{-6} K^{-1} for a Si substrate) is two orders of magnitude smaller than the thermo-optic coefficient for silicon, it can be omitted as well [26], leaving the commonly reduced expression,

$$\frac{d\lambda}{dT}=\frac{\partial n_{eff}}{\partial T}\frac{\lambda_0}{n_g} \quad (2)$$

The repercussions of resonance shifts on microring functionality will be dependent on the quality factor (Q) of the resonance. However, for typical applications, deviations in temperature >1 K will render the microring-based device inoperable [27]. This susceptibility of microring-based devices is not compatible with the temperature ranges typical of microelectronic environments. It should be clarified that it is not the absolute temperature that is hazardous for microring-functionality; rather, it is the relative changes in temperature during active operation of the optical link.

Resolutions to this problem can be classified into two categories: 1) solutions that reduce the thermal dependence of the microring resonator (denoted as "athermal" solutions), and 2) solutions that actively maintain the local temperature of the microring resonator (denoted as "control-based" solutions). In general, a significant advantage of athermal solutions is that they require no active power consumption to implement. The disadvantages of athermal solutions is their difficult fabrication, either though the incorporation of non-CMOS materials, or additional photonic structures. In contrast, the only additional structures that control-based systems typically require are integrated heaters and photodetectors, elements that are readily available in a typical silicon photonic platform. However, the main disadvantage of control-based systems is their active power consumption.

Before committing to either class of solutions, further system analysis must be given consideration. Specifically, the laser sources driving the optical link must be evaluated. Currently, in commercial telecommunications links, laser wavelengths are kept locked to a fixed wavelength grid (the ITU standard). However, for the future short-reach interconnects that silicon-photonic devices are envisioned to populate, a different class of low-power laser sources will be required [19, 28–30]. For athermal solutions, it will be required that laser wavelengths are fixed to the resonant wavelengths of the microring resonators, and that the stability of the laser wavelength can be ensured throughout operation of the optical link. In contrast, for control-based solutions no such constraints are needed for the initial wavelengths of the laser source, or for guaranteeing wavelength stability. Fluctuations in wavelength are analogous to fluctuations in temperature; any control system that corrects for temperature changes will correspondingly be able to correct for fluctuations in wavelength as well. Ultimately, when considering the larger system design, any power required to stabilize the laser source must be included when weighing the advantages and disadvantages of these two classes of solutions.

3 Athermal devices

The goal of athermalizing silicon microring-based devices is to significantly decrease the temperature-dependence of the microring resonance (the use of the term "athermal" is somewhat of a misnomer because the temperature dependence is never completely eliminated, just reduced to a tolerable level). The two dominant techniques for achieving athermalization is the use of materials with negative thermo-optic coefficients (silicon has a positive thermo-optic coefficient) in waveguide claddings, and embedment of the microring in a thermally balanced interferometer.

3.1 Athermalization using negative thermo-optic materials

The concept of using a negative thermo-optic polymer cladding for the athermalization of optical waveguides was first introduced by Kokobun et al. [31], and has since been adapted to silicon microring resonators. The goal of this technique is to produce an aggregate thermo-optic coefficient for the waveguide which is zero, with the thermo-optic coefficient defined as

$$\frac{\partial n_{eff}}{\partial T}=\Gamma_{core}\frac{\partial n_{core}}{\partial T}+\Gamma_{cladding}\frac{\partial n_{cladding}}{\partial T}+\Gamma_{substrate}\frac{\partial n_{substrate}}{\partial T} \quad (3)$$

where Γ is the modal confinement factors for the core, cladding, and substrate, as specified [32]. The modal confinement and negative thermo-optic coefficient of the cladding are engineered to balance the modal confinement and positive thermo-optic coefficients of the core (silicon) and substrate (silicon dioxide). It should be noted that the wavelength dependency is not denoted in Eq. (3), and furthermore, only linear terms have been included. Higher-order wavelength dependencies of the thermo-optic coefficient make it difficult to achieve athermal behavior over a broad wavelength and temperature range [32, 33].

The high thermo-optic coefficient and modal confinement of silicon waveguides makes it difficult to balance Eq. (3) such that the net thermo-optic coefficient is zero. In addition to finding a polymer with a negative thermo-optic coefficient of the same magnitude as silicon's, it is necessary to re-engineer the optical mode such that it is more distributed in the polymer cladding (a larger $\Gamma_{cladding}$). Demonstrated methods to achieve this have involved narrowing or thinning the waveguide, or utilizing a slotted structure [24, 26, 34–36]. Figure 3A depicts a typical cross-section of polymer-clad silicon waveguide. As the waveguide is narrowed or thinned, more of the optical mode is distributed in the polymer cladding. Figure 3B quantitatively shows this relationship, and identifies a waveguide dimension for which Eq. (3) balances for a particular wavelength and polymer cladding. In particular, this design was able to reduce the temperature dependent resonance shift (TDWS) to -5 pm/K over a range of 50 K [24]. More recent work has established TDWS as low as 0.2 pm/K [33].

The strict requirement on waveguide dimensions may make it difficult to consistently achieve the desired athermalization given the natural variations present in fabricating silicon photonic structures. A possible resolution to this issue is to use photosensitive materials, such as chalcogenide glasses, to enable the thermo-optic coefficient to be trimmed post-fabrication as necessary [37–39].

In addition to the difficulty in precisely tuning the thermo-optic coefficient of polymers, additional consideration must be given to their compatibility with the CMOS-fabrication processes that are envisioned for the future production of silicon photonic platforms. In particular, polymers are vulnerable to degradation, especially when exposed to high temperatures, as would exist in certain stages of a typical CMOS-production cycle [40]. Additionally, polymers suffer from chemical instability, UV aging, and poor mechanical characteristics [41].

Given these detrimental characteristics of polymers, recent research has focused on the use of titanium dioxide (TiO_2) for use as a negative thermo-optic coefficient

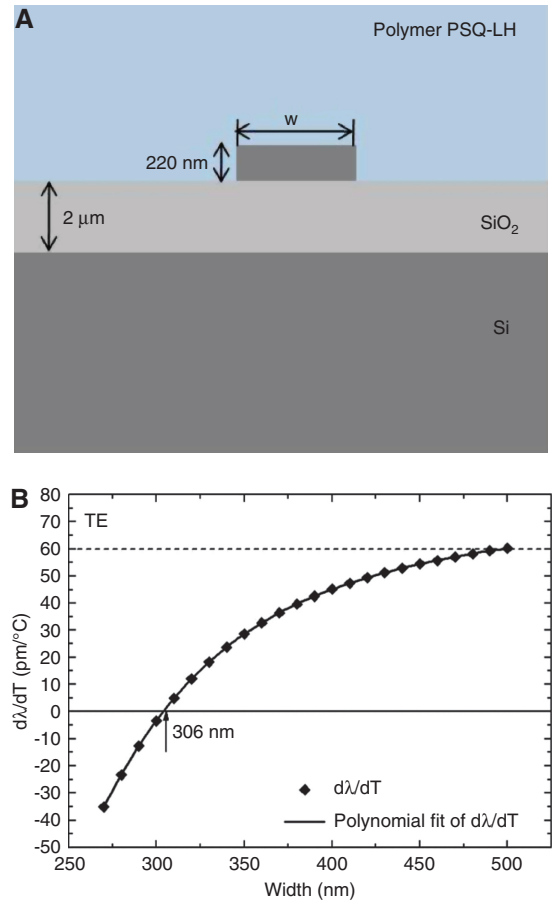

Figure 3 (A) cross-section of a SOI waveguide with polymer overlay. (B) Calculated wavelength temperature dependence of the TE mode as a function of waveguide widths. Reprinted with permission from Ref. [24], copyright (2009) OSA.

cladding material [41–44] TiO_2 is one of the few CMOS-compatible materials that has a negative thermo-optic coefficient (~-1.8×10^{-4} K^{-1}) on the same order as Si [42]. TiO_2-clad silicon microring resonators have been demonstrated to have a TDWS <2 pm/K over a range of 5 K, and importantly, have been shown to be capable of current-injection induced resonance shifts (necessary for high-speed modulation) [43].

The aforementioned results show that negative thermo-optic coefficient materials can be effectively used to drastically reduce the thermal susceptibility of silicon microring resonators, making them appropriate for applications in microelectronics. However, the difficulty in the solution lies in the incorporation of said materials, whether polymer or TiO_2, into a CMOS compatible fabrication process. Additionally, these configurations must be able to fall within the fabrication tolerances of said processes (or able to be tuned post-fabrication). Finally, it should be noted that the required reduction in the modal

confinement of the core will have consequences on the losses of the microring in straight and bent configurations, negatively impacting such desired attributes as footprint and Q-factor [32].

3.2 Athermalization using an interferometric structure

An alternative to using negative thermo-optic materials is to embed the microring resonator in a thermally matched mach-zhender interferometer (MZI). It has been shown that a silicon MZI can be athermalized by engineering the optical modes in each arm of the MZI. Specifically, the width of the waveguides in the MZI is varied so that the guided mode in each arm of the MZI experiences a different effective thermo-optic coefficient. This is balanced against the length of the arms to produce an overall athermal optical response for the MZI filter [45, 46]. It is possible to adapt this technique to microring resonators by embedding the resonator in one arm of the MZI, as seen in Figure 4A [47].

Figure 4C shows that the structure can be designed such that the thermal sensitivity of the microring resonator cancels the thermal sensitivity of the MZI it is embedded in. However, because the dependence of the phase shift of the MZI with respect to temperature is linear, whereas is it nonlinear for the microring resonator, the resultant optical resonance will slightly deviate and deform across a given temperature range [47]. By embedding a diode structure in the microring (a typical configuration) it has been shown that this device can be utilized as an athermal high-speed electro-optic modulator [48]. Figure 5 shows simulated and measured eye diagrams from said device. As is expected, the slight deformation and deviation in the MZI-embedded microring resonator's optical response across the temperature range sometimes yields atypical electro-optic modulation, albeit, this may be sufficient for some applications.

The advantage of this technique is clear, the introduction of the thermally balanced MZI structure does not require the incorporation of any new layers or materials in the fabrication of the silicon photonic structure. In contrast to the athermal solutions utilizing a negative thermo-optic material, this solution can be readily integrated using current CMOS-fabrication techniques. However, the structure still suffers from susceptibility to fabrication tolerances, and furthermore, increases the footprint of the microring structure. Additionally, it is non-trivial to adapt the technique to larger microring switch fabrics [15].

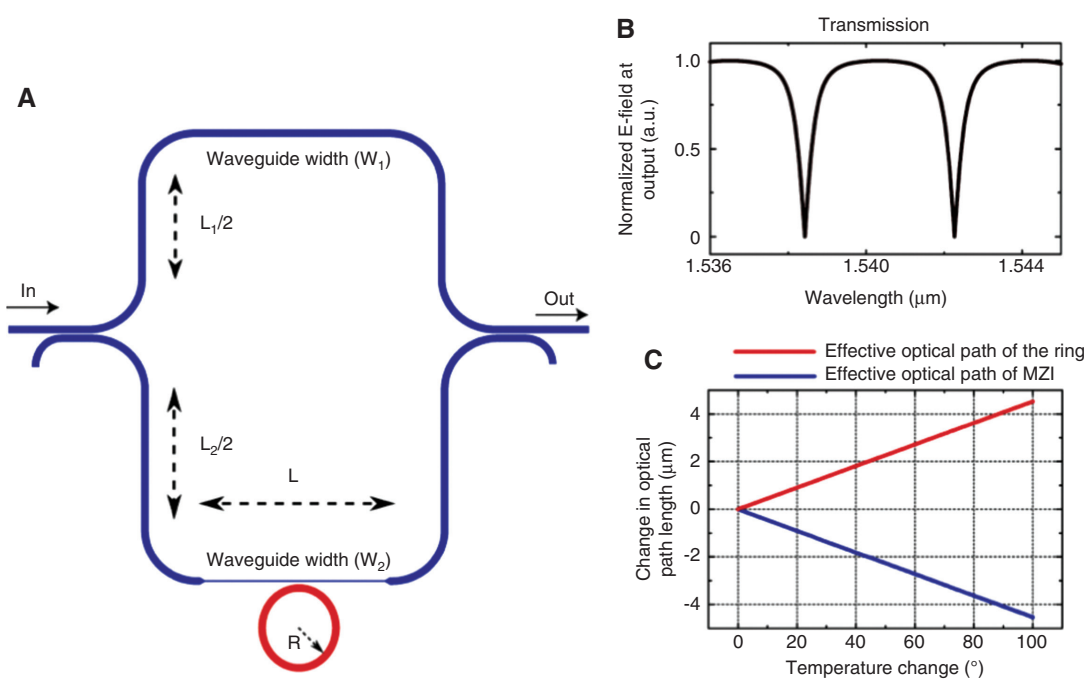

Figure 4 (A) Schematic of a microring resonator embedded in a thermally engineered MZI, showing the various waveguide lengths and widths. The MZI is highlighted in blue and the microring in red. (B) Typical transmission spectrum for such a device with a 40 μm microring radius. (C) Change in optical path length with temperature for the microring and MZI. The devices are designed to have opposite and equal phase shifts with increase in temperature. Reprinted with permission from Ref. [47] copyright (2010) OSA.

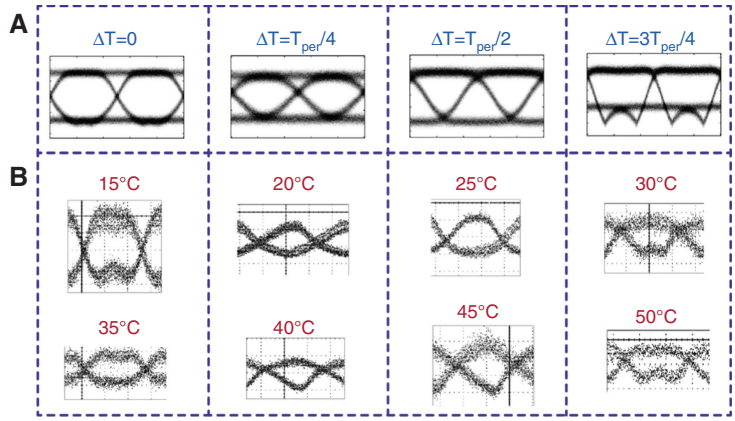

Figure 5 (A) Simulated eye diagrams showing the periodic change in eye diagram shape with temperature over one temperature period. (B) 2 Gb/s square wave modulation eye diagrams for different temperatures. Measurements span over two temperature periods. Corresponding predicted eye is shown in the top row. Reprinted with permission from Ref. [48], copyright (2012) OSA.

4 Control-based solutions

While athermal solutions work by removing the thermal sensitivity of silicon microring resonators, control-based solutions operate by maintaining the local temperature of the microring resonator throughout the duration of its operation. This is accomplished through the use of an integrated heater localized to the microring resonator. Because cooling solutions (such as peltier coolers) are prohibitively power inefficient, there is no practical method to effectively cool microring resonators. Rather, leveraging the repeated nature of the microring's optical resonances, the predominant solution is to use integrated heaters to "run the microring hot" during the system initialization. Subsequent decreases or increases in environmental temperature can then be corrected for by increasing and decreasing, respectively, the power delivered to the integrated heater.

In its generalized form, as depicted in Figure 6, control systems require a method to monitor the temperature drift of the microring resonator, a feedback controller to condition the response, and a method to adjust the local temperature of the microring resonator (the integrated heater).

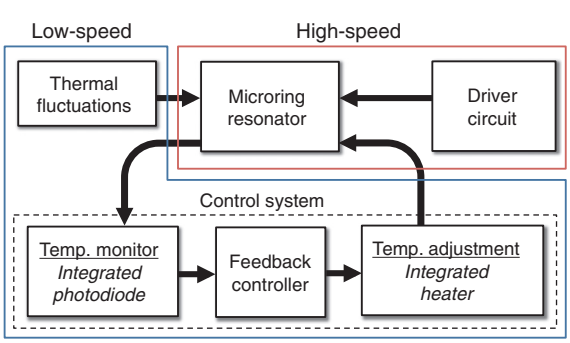

Figure 6 Generalized scheme for control-based solutions, emphasizing the separation between the low-speed thermal stabilization and the high-speed electrical operation (in the case of a modulator or switch) of the microring resonator.

In essence, there are two major components to any control-based solution, the integrated heater controlling the local temperature of the microring resonator, and the control-system driving the integrated heater. The characteristics of each of these components, including the power consumption and ease of implementation, can be analyzed separately.

4.1 Integrated heaters

Integrated heaters are resistive elements and are typically constructed from nichrome, titanium, or doped silicon materials. Running current through these resistive structures generates heat, which can be used to tune the local temperature of the microring resonator. A noted alternative, available for carrier-injection microring modulators, is to adjust the bias current of the diode junction to directly heat the microring resonator [27, 49, 50]. This technique was used to implement the first control system for thermally stabilizing a microring resonator for data applications [27]. However, while effective, bias tuning has a limited temperature tuning range [49], and was found to have deleterious effects on the generated optical modulation [27]. The preferred solution is to use an integrated heater to separate the high-speed electrical operation of the microring resonator from its (relatively) low-speed thermal stabilization.

The critical metrics for integrated heaters are their tuning efficiency and their tuning speed. While the tuning

efficiency is typically given in (mW/nm) or (mW/GHz), a more universal metric is to express the tuning efficiency as the power required to tune the microring resonator by one free-spectral-range (FSR). The (mW/nm) metric increases with increasing microring size, however, because the FSR of the microring also correspondingly decreases, the (mW/FSR), also denoted as (mW/2π), will remain relatively constant across varying microring sizes [51]. This is useful for comparing tuning efficiency results of integrated heaters on microring resonators of different sizes.

The cross-sections in Figure 7, depicts the normal configuration for integrated heaters, whereby a thermally grown SiO_2 layer of ~1 μm separates the metal heater from the silicon waveguide [15]. The separation between the heater and silicon waveguide is required to protect the optical mode (Figure 7A). The tuning efficiency is not optimal as a consequence of the separation, as the generated heat has to diffuse from the point-like source of the heater down to the silicon waveguide (Figure 7B). While this configuration is the easiest to implement in fabrication, demonstrated tuning efficiencies are limited, with most results ranging around ~100 mW/FSR [15, 52–54], and the best demonstration at ~42 mW/FSR with a tuning speed of 14 μs [55]. These tuning efficiencies may be sufficient for some applications, but for the applications with the most stringent requirements on interconnect power consumption an improved tuning efficiency will be required. Demonstrations have shown that the tuning efficiency can be improved by either locating the integrated heater closer to the microring resonator or by improving the thermal isolation of the microring.

There is an inherent difficulty of locating the integrated heater closer to the microring resonator without causing the optical mode to incur additional scattering loss. A solution to resolving this problem is to utilize a microdisk resonator (functionality equivalent to a microring resonator) and place the integrated heater within the interior of the resonator. However, microdisk structures also support additional optical modes which corrupt the FSR of the resonator. The use of adiabatic microring resonators merges the benefits of microring and microdisk structures, allowing interior connections to the resonator while suppressing spurious optical modes and maintaining a small footprint [56]. Figure 8A depicts the form factor of an adiabatic microring resonator, and the direct integration of a heater within the resonator (Figure 8B). Leveraging the intimate placement of the heater, tuning powers as low as ~20 mW/FSR with tuning speeds as fast as ~1 μs were demonstrated [57]. Additionally, it was shown that adiabatic microring modulators could be fabricated [58]. Modulators with interior integrated heaters have been shown to be able to produce error-free 10 Gb/s modulation across a 60 K temperature tuning range, with comparable tuning efficiencies [59].

Another method to improve the tuning efficiency of integrated heaters is to increase the thermal isolation of microring resonators. Ordinarily, much of the heat generated by the integrated heater is dissipated into the surrounding oxide and substrate. To prevent this, air trenches can be etched around the resonator structure, increasing its thermal isolation from the surrounding environment (Figure 9A). Using this technique, tuning powers of 21 mW/FSR with tuning time constants <10 μs were demonstrated [61].

Further improvements in tuning efficiency can be obtained by completely thermally isolating the resonator structure from the silicon substrate (Figure 9B) The particulars of the nanofabrication technique to achieve this physical isolation differ, and can utilize either topside silicon undercut-etching [25, 60], or backside

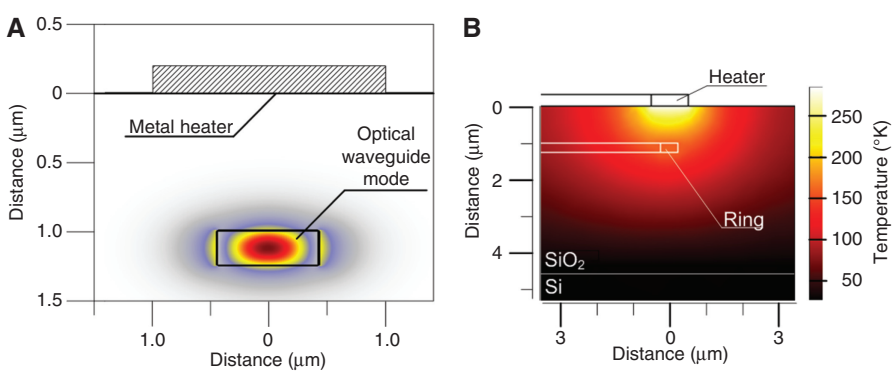

Figure 7 Heater and waveguide design for thermal and optical efficiency: (A) the optical mode is separated from the heater to avoid absorption while (B) maintaining enough proximity to couple heat into the waveguide. Reprinted with permission from Ref. [15], copyright (2008) OSA.

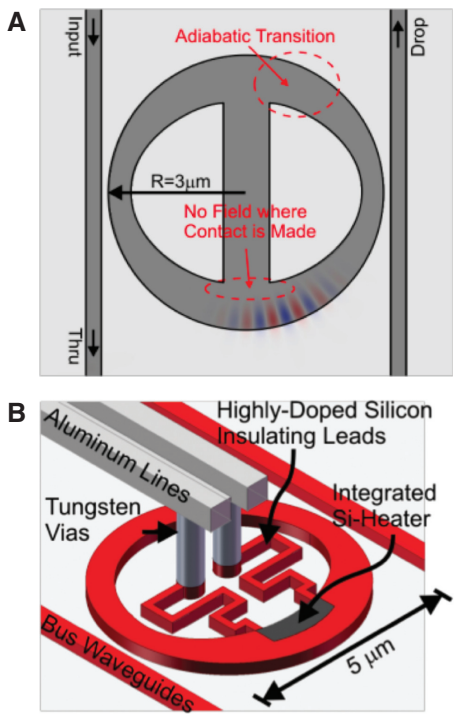

Figure 8 (A) FD-TD simulation of an adiabatic microring resonator. (B) Diagram of an adiabatic microring resonator with integrated heaters. Reprinted with permission from Ref. [57], copyright (2009) OSA.

substrate etching [51]. When isolated from the substrate, tuning powers of 2.4 mW/FSR [60], 3.9 mW/FSR [51], and 4.9 mW/FSR [25] were demonstrated, a magnitude of order improvement in tuning efficiency.

These record-breaking results in tuning efficiency are ideal for applications where microring-based devices have to abide by strict power consumption requirements. However, the etch removal of the substrate may not be compatible with certain silicon photonic implementations, albeit, impressive progress has been made in extending undercut structures to larger scales [62]. Additionally, a consequence of the thermal isolation is that the thermal time constant is drastically increased, as high as ~170 μs [60]. This may not be a critical parameter however, as environmental temperature fluctuations are likely to be above the ~ms regime [63], making undercut integrated heaters appropriate for thermal stabilization systems. However, it should be noted that increasing the thermal impedance of the microring resonator renders it more susceptible to optical bistability effects, which can have deleterious effects on microring modulation [64, 65].

4.2 Methods for control-based solutions

In order for an integrated heater to effectively stabilize the temperature of a microring resonator it must be interfaced with control circuitry. In addition to thermally stabilizing the microring resonator, this control circuitry should be able to initialize the optical link by aligning the relevant microring resonators with their corresponding laser wavelengths (a process known as wavelength-locking).

The general scheme of this control system would be to utilize some sensing mechanism to ascertain thermal drifts in the microring, denoted as an error signal, and a close-looped feedback controller to condition the error and adjust the voltage on the integrated heater. The feedback controller in any implemented control system is likely to be some digital or analog manifestation of a proportional-integral-derivative (PID) controller, a robust and simple method of achieving closed-loop feedback control [27]. However, there is no clear consensus as to what the best method to monitor the drift of the microring resonator is. The ideal solution is one that is low-cost and energy-efficient, does not require additional photonic structures, is compatible with the WDM implementation of microring resonators, immune to fluctuations in laser power, and implementable for either passive microring resonators or active components such as microring modulators.

Direct monitoring of the microring resonator temperature has been demonstrated [58], however, temperature sensors may be too slow and they have not yet been demonstrated working successfully in a control system. Rather, the predominant solutions rely on

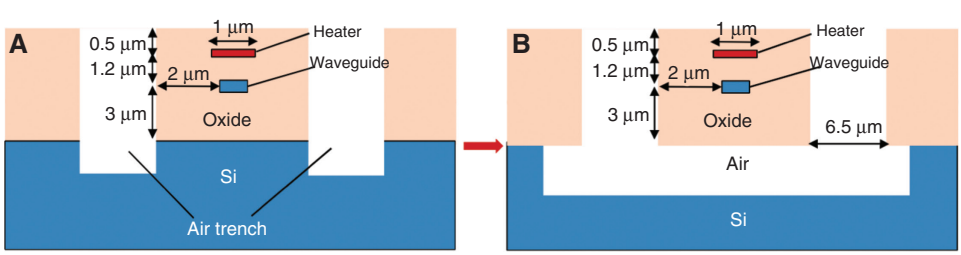

Figure 9 (A) Cross section of the resonator waveguide with air trenches. (B) Cross section of the resonator waveguide with undercuts beneath the waveguides. Reprinted with permission from Ref. [60], copyright (2010) OSA.

indirectly monitoring drifts in the microring resonator. For instance, one example utilizes an infrared camera to image scattered light, however, this method will likely be difficult to scale and implement in a cost-effective and compact manner [66].

Several methods utilize the optical power of the signal to infer drifts in the microring resonator. It was shown that wavelength-locking and stabilization could be achieved by algorithmically searching for the point of minimum power transmission of a passive microring resonator [67]. While effective, it remains to be seen whether the FPGA-implementation can be translated to simple low-power circuitry, and additionally, the technique may be vulnerable to fabry-perot artifacts in the optical path.

Additionally, it has been shown that monitoring the optical power of the generated data signal is sufficient for stabilizing microring modulators [27]. This technique relies on the fact that an on-off-keyed (OOK) signal will have a lower mean power than a non-modulated signal. Figure 10 illustrates this by mapping the wavelength spectrum (on a drop-port photodiode) of the modulated waveform with its corresponding eye diagrams. Monitoring the optical signal on the drop port of the microring modulator eliminates the need for a power tap and yields the system WDM compatibility [68]. This method was shown to maintain the error-free performance of a microring modulator amidst thermal fluctuations that would normally render it inoperable. Monitoring the mean modulated power is an effective method because it can be implemented using low-speed (and hence low-cost and energy-efficient) circuitry and a low-speed, weak photodiode. However, it is susceptible to fluctuations in laser power and is not applicable to passive resonators.

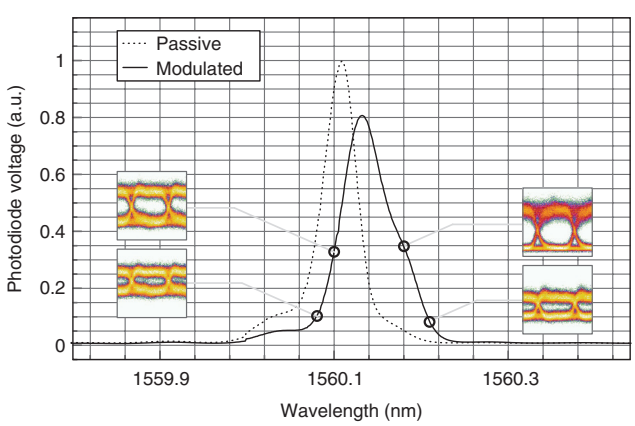

Figure 10 Measured photoresponse of the drop-port photodiode for when the microring is in its passive state, as well as for when it is modulated. Generated 5-Gb/s eye diagrams are indicated at several points on the measured photoresponse of the modulated microring.

A departure from monitoring the mean modulated power of the signal is to directly monitor the bit-error-rate (BER) of the generated data stream [69]. Demonstrated results showed wavelength locking and thermal stabilization of the modulator over a range of 32 K. By directly monitoring and optimizing the BER of the modulator the method controls microring modulator drift according to the most important application metric: the quality of the generated data. However, in contrast to optical power monitoring [68], monitoring of the BER is much more complex, requiring more circuitry (operating at a speed equivalent to the generation of the data) and high-speed receivers. This has consequences on the ease of implementation and overall power-consumption of the system. In addition, like [68], this method is only applicable to microring modulators, not microrings implemented as switches or filters.

The difficulty in finding an efficient and straightforward method for wavelength-locking and stabilizing resonators is a result of the symmetry of the microring's optical resonance. A similar engineering problem is faced when the locking the wavelength of a laser to a fixed reference gas cavity, which also possesses a symmetrical optical resonance. For that scenario, the common and established method has been to create an anti-symmetric error signal (a derivative of the optical response) centered about the resonant wavelength [70]. Similarly, the generation of an anti-symmetric error signal would greatly ease the task of locking and stabilizing microring resonators.

One method to produce this desired error signal is to place the microring in an interferometric structure and utilize homodyne detection [71]. While meeting many metrics of the ideal solution, such as its simplicity and WDM compatibility, the introduction of the interferometric structure may be difficult to implement with some configurations of microring resonators, such as more complicated microring switch routers [15].

An alternative for generating the anti-symmetric error signal is to use a dithering signal [72]. Figure 11 illustrates the concept of dithering, whereby a small modulation is applied to the resonator to produce a small modulation

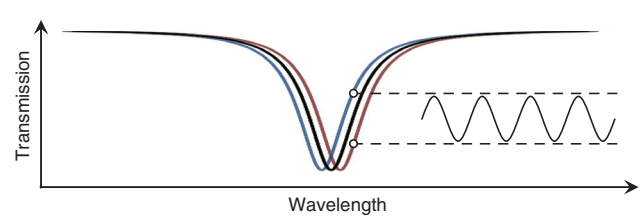

Figure 11 A small dither signal, applied thermally or electrically to the microring resonator, results in a small modulation of the optical signal.

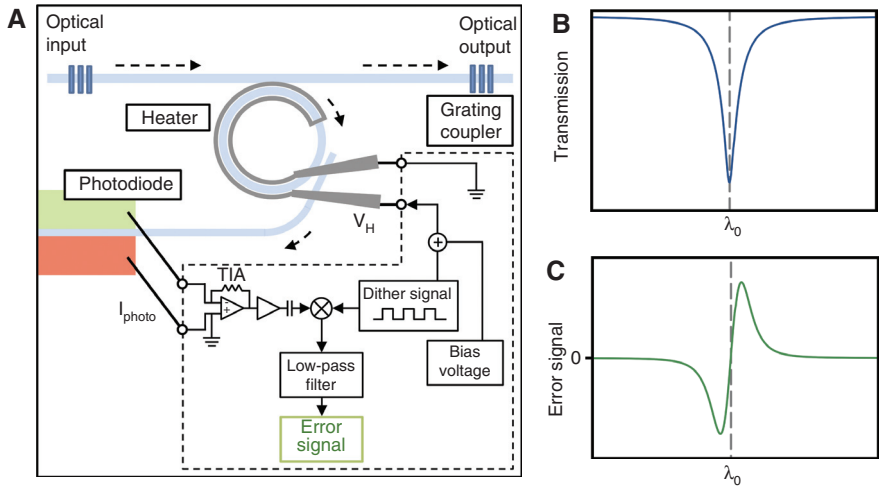

Figure 12 (A) An implementation of using a dithering signal to generate an anti-symmetric error signal. (B) The optical resonance of the microring resonator. (C) The anti-symmetric error signal.

of the optical signal. The generated signal will either be in-, or out-of-phase with the driving signal, depending on which side of the resonance the laser is offset. By mixing the modulated optical signal with the driving dithering signal this information can be recovered as shown in Eq. (4), where f_D is the frequency of the dithering signal, and ϕ is the relative phase (0 or π) of the modulated optical signal.

$$\cos(f_D t)\otimes\cos(f_D t+\phi)=\frac{1}{2}[\cos(2f_D t+\phi)+\cos(\phi)] \tag{4}$$

The higher harmonic can be filtered, leaving the sign of the DC component {cos(ϕ) term} as an indication of the location of the resonance relative to the optical signal. Figure 12 depicts the experimental implementation when applying the dithering signal thermally. With a thermal dithering magnitude as small as 0.1 K, and as slow as 1-kHz, it is possible to wavelength lock and thermally stabilize a passive microring resonator. A consequence of the dithering is an intrinsic reduction in the extinction ratio of the microring resonator, however, this was shown to be relatively small and the impact on the performance of the microring should be negligible [72].

The use of a dithering signal has several advantages over the previous methods. It may be one of the simplest methods to implement as it relies on low-speed and power-efficient circuitry. It is immune against fluctuations in laser power, compatible with WDM configurations, and robust against fabry-perot artifacts. Most importantly, it does not require additional photonic structures, making it readily implementable on more complicated microring structures, utilizing either drop-port photodiodes or *in-situ* waveguide photodetectors [73]. While current demonstrations show the utility of anti-symmetric error signals for passive microring resonators, methods can be developed to adapt them to microring modulators as well [71].

5 Conclusion

We have comprehensively surveyed the current athermal and control-based solutions for resolving the thermal challenges facing microring-based devices. While the zero-power consumption characteristic of athermal solutions is ideal, their difficulty in nanofabrication and/or incorporation of non-CMOS materials may prevent them from ever proliferating within a large-scale silicon photonics platform. Additionally, a full system analysis would have to give consideration to the power required to thermally stabilize the laser source, as athermal devices will only work on a rigidly fixed wavelength grid.

Control-based solutions have demonstrated the full gambit of functionality, showing the ability to wavelength-lock and thermally stabilize both passive and active microring-based devices. However, a major concern lies in their active power consumption, which may possibly null the benefits in energy-efficiency achieved by using microring-based devices. An energy-efficient control-based solution will require that both the circuitry and the integrated heater have low active power consumption.

When implemented in proper CMOS circuitry it is likely that the power consumption of the control system can be reduced to a sufficient level. For example, for the method utilizing power monitoring [68], it is forecasted that a CMOS implementation would have a ~25 fJ/bit

power consumption (at a 10 Gb/s data rate). CMOS implementation of the dithering method [72] would require building further upon this circuitry, but likely keep power consumption below 100 fJ/bit. Similarly, it is forecasted that the BER monitoring method [69] would consume only 55 fJ/bit (at 10 Gb/s).

Of significant concern is the power consumption of the integrated heaters. If it is indeed required to tune microring resonators over a full FSR the integrated heaters would be the dominant source of power consumption in the optical link. However, current system designs suggest that such large tuning ranges are unnecessary. Advances in silicon photonic fabrication have been able to control wafer and etch tolerances to produce relatively evenly spaced WDM microring arrays [74]. In evenly channel-spaced WDM microring arrays, no microring will need to be initially tuned beyond one channel spacing length. In addition, following large temperature swings, channel assignments can be reshuffled to minimize the aggregate tuning needed [21], potentially reducing the required power consumption of the integrated heaters to values <100 fJ/bit (at 10 Gb/s) [69]. More accurate estimates of power consumption may only arrive with further progress in the development and implementation of control systems. However, another consideration that requires equal attention are the temperature parameters of the environment, specifically the magnitude and bandwidth of thermal fluctuations afflicting microring-based devices [63]. Better definition of these parameter-bounds will enable a more accurate assessment of the power-consumption of control systems.

Received May 13, 2013; accepted August 12, 2013; previously published online September 11, 2013

References

[1] Krishnamoorthy AV, Ho R, Zheng X, Schwetman, H. Computer systems based on silicon photonic interconnects. Proc IEEE 2009;97(7):1337–61.
[2] Urata R, Liu H, Lam C, Dashti P, Johnson C. Silicon photonics for optical access networks. Proc IEEE Group IV Photonics, San Diego, CA, 2012:207–9.
[3] Lee BG, Plouchart J, Rylyakov AV, Song JH, Doany FE, Schow CL. Passive photonics in an unmodified CMOS technology with no post-processing required. IEEE Photonic Tech L 2013;25(4):393–6.
[4] Dong P, Qian W, Liao S, Liang H, Kung CC, Feng NN, Shafiiha R, Fong J, Feng D, Krishnamoorthy AV, Asghari M. Low loss shallow-ridge silicon waveguides. Opt Express 2010;18(14):14474–9.
[5] Xu F, Poon AW. Silicon cross-connect filters using microring resonator coupled multimode-interference-based waveguide crossings. Opt Express 2008;16(12):8649–57.
[6] Green WMJ, Rooks MJ, Sekaric L, Vlasov YA. Ultra-compact, low RF power, 10 Gb/s silicon Mach-Zhender modulator. Opt Express 2007;15(25):17106–13.
[7] Cheung STS, Guan B, Djordjevic SS, Okamoto K, Yoo SJB. Low-loss and high contrast silicon-on-insulator (SOI) arrayed waveguide grating. Proc Conference on Lasers and Electro-Optics, San Jose, 2012.
[8] Grote RR, Padmaraju K, Driscoll JB, Souhan B, Bergman K, Osgood R. 10 Gb/s Error-free operation of all-silicon ion-implanted-waveguide photodiodes at 1.55μm. IEEE Photonic Tech L 2013;25(1):67–70.
[9] Assefa S, Xia F, Bedell SW, Zhang Y, Topuria T, Rice PM, Vlasov YA. CMOS-integrated high-speed MSM germanium waveguide photodetector. Opt Express 2010;18(5):4986–99.
[10] Xu Q, Fattal D, Beausoleil RG. Silicon microring resonators with 1.5-μm radius. Opt Express 2008;16(6):4309–15.
[11] Xu Q, Schmidt B, Pradhan S, Lipson M. Micrometre-scale silicon electro-optic modulator. Nature 2005;435:325–7.
[12] Pantouvaki M, Yu H, Rakowski M, Christie P, Verheyen P, Lepage G, Van Hoovels N, Absil P, Van Campenhout J. Comparison of silicon ring modulators with interdigitated and lateral PN junctions. IEEE J Sel Top Quant 2013;19(2): Article ID: 7900308.
[13] Chen L, Lipson M. Ultra-low capacitance and high-speed germanium photodetectors on silicon. Opt Express 2009;17(10):7901–6.
[14] Biberman A, Lira HLR, Padmaraju K, Ophir N, Chan J, Lipson M, Bergman K. Broadband silicon photonic electrooptic switch for photonic interconnection networks. IEEE Photonic Tech L 2011;23(8):504–6.
[15] Sherwood-Droz N, Wang H, Chen L, Lee BG, Biberman A, Bergman K, Lipson M. Optical 4×4 hitless silicon router for optical Networks-on-Chip (NoC). Opt Express 2008;16(20):15915–22.
[16] Li G, Zheng X, Yao J, Thacker H, Shubin I, Luo Y, Raj K, Cunningham JE, Krishnamoorthy AV. 25Gb/s 1V-driving CMOS ring modulator with integrated thermal tuning. Opt Express 2011;19(21):20435–43.
[17] Xiao X, Xu H, Li X, Li Z, Chu T, Yu J, Yu Y. 60 Gbit/s Silicon modulators with enhanced electro-optical efficiency. Proc Optical Fiber Communication Conference, Anaheim, 2013.
[18] Lee BG, Small BA, Xu Q, Lipson M, Bergman K. Characterization of a 4×4 Gb/s parallel electronic bus to WDM optical link silicon photonic translator. IEEE Photonic Tech L 2007;19(7):456–8.
[19] Ophir N, Mountain D, Mineo C, Bergman K. Silicon photonic microring links for high-bandwidth-density, low-power chip I/O. IEEE Micro 2013;33(1):54–67.
[20] Ayazi A, Baehr-Jones T, Liu Y, Lim AEJ, Hochberg M. Linearity of silicon ring modulators for analog optical links. Opt Express 2012;20(12):13115–22.
[21] Georgas M, Leu J, Moss B, Sun C, Stojanovic V. Addressing link-level design tradeoffs for integrated photonics

interconnects. Proc IEEE Custom Integrated Circuits Conference, 2011.
[22] Preston K, Sherwood-Droz N, Levy JS, Lipson M. Performance guidelines for WDM interconnects based on silicon microring resonators. Proc Conference on Lasers and Electro-Optics, 2011.
[23] Magdalena SN, Tao L, Xuan W, Robert RP. Tunable silicon microring resonator with wide free spectral range. Appl Phys Lett 2006;89: Article ID: 071110.
[24] Teng J, Dumon P, Bogaerts W, Zhang H, Jian X, Han X, Zhao M, Morthier G, Baets R. Athermal silicon-on-insulator ring resonators by overlaying a polymer cladding on narrowed waveguides. Opt Express 2009;17(17):14627–33.
[25] Fang Q, Song J, Luo X, Jia L, Yu M, Lo G, Liu Y. High efficiency ring-resonator filter with NiSi heater. IEEE Photonic Tech L 2012;24(5):350–2.
[26] Alipour P, Hosseini ES, Eftekhar AA, Momeni B, Adibi A. Athermal performance in high-Q polymer-clad silicon microdisk resonators. Opt Lett 2010;35(20):3462–4.
[27] Padmaraju K, Chan J, Chen L, Lipson M, Bergman K. Thermal stabilization of a microring modulator using feedback control. Opt Express 2012;20(27):27999–8008.
[28] Knights AP, Huante-Ceron E, Ackert J, Logan D, Wojcik G, Zhang F, Gubenko A, Mikhrin S. Comb-laser driven WDM for short reach silicon photonic based optical interconnection. Proc IEEE Group IV Photonic, San Diego, CA, 2012:210–2.
[29] Livshits D, Livshits D, Gubenko YA, Krestnikov I, Mikhrin S, Kovsh A, Wojcik G. Cost-effective WDM optical interconnects enabled by quantum dot comb lasers. Proc Optoelectronic Interconnects and Component Integration IX, Vol. 7606, San Francisco, CA, 2010.
[30] Levy JS, Saha K, Okawachi Y, Foster MA, Gaeta AL, Lipson M. High-performance silicon-nitride-based multiple-wavelength source. IEEE Photonic Tech L 2012;24(16):1375–7.
[31] Kokobun Y, Funato N, Takizawa M. Athermal waveguides for temperature-independent lightwave devices. IEEE Photonic Tech L 1993;5(11):1297–300.
[32] Raghunathan V, Ye W, Hu J, Izuhara T, Michel J, Kimerlin L. Athermal operation of Silicon waveguides: spectral, second order and footprint dependencies. Opt Express 2010;18(17):17631–9.
[33] Milosevic MM, Gardes FY, Thomson DJ, Mashanovich GZ. Temperature insensitive racetrack resonators for near infrared applications. Proc Optical Fiber Communication Conference, Los Angeles, 2012.
[34] Lee J-M, Kim D-J, Ahn H, Kim S-H, Park G. Temperature dependence of a silicon nanophotonic ring resonator with a polymeric overlayer. J Lightwave Technol 2007;25(8):2236–43.
[35] Zhou L, Kashiwagi K, Okamoto K, Scott RP, Fontaine NK, Ding D, Akella V, Yoo SJB. Towards athermal optically-interconnected computing system using slotted silicon microring resonators and RF-photonic comb generation. Appl Phys A 2009;95:1101–9.
[36] Li Q, Yegnanarayanan S, Soltani M, Alipour P, Adibi A. A temperature-insensitive third-order coupled-resonator filter for on-chip terabit/s optical interconnects. IEEE Photonic Tech L 2010;22(23):1768–70.
[37] Raghunathan V, Grillanda S, Singh V, Canciamilla A, Morichetti F, Agarwal A, Michel J, Melloni A, Kimerling LC. Trimming of athermal silicon resonators. Proc Integrated Photonics Research, Silicon and Nanophotonics, Colorado Springs, CO, 2012.
[38] Qiu F, Yu F, Spring AM, Yokoyama S. Athermal silicon nitride ring resonator by photobleaching of disperse red 1-doped poly(methyl methacrylate) polymer. Opt Lett 2012;37(19):4086–8.
[39] Zhou L, Okamoto K, Yoo SJB. Athermalizing and trimming of slotted silicon microring resonators with UV-sensitive PMMA upper-cladding. IEEE Photonic Tech L 2009;21(17):1175–7.
[40] Raghunathan V, Izuhara T, Michel J, Kimerling L. Stability of polymer-dielectric bi-layers for athermal silicon photonics. Opt Express 2012;20(14):16059–66.
[41] Shang K, Djordjevic SS, Li J, Liao L, Basak J, Liu H-F, Ben Yoo SJ. CMOS-compatible titanium dioxide deposition for athermalization of silicon photonic waveguides. Proc Conference on Lasers and Electro-Optics, San Jose, 2013.
[42] Zhu S, Lo GQ, Xie J, Kwong DL. Towards athermal nanoplasmonic resonators based on Cu-TiO2-Si hybrid plasmonic waveguide. Proc Optical Fiber Communication Conference, Anaheim, 2013.
[43] Djordjevic SS, Shang K, Guan B, Cheung ST, Liao L, Basak J, Liu HF, Yoo SJ. CMOS-compatible, athermal silicon ring modulators clad with titanium dioxide. Opt Express 2013;21(12):13958–68.
[44] Alipour P, Atabaki AH, Eftekhar AA, Adibi A. Athermal performance in titania-clad microresonators on SOI. Proc Frontiers in Optics, Rochester, NY, 2010.
[45] Uenuma M, Mooka T. Temperature-independent silicon waveguide optical filter. Opt Lett 2009;34(5):599–601.
[46] Guha B, Gondarenko A, Lipson M. Minimizing temperature sensitivity of silicon Mach-Zhender interferometers. Opt Express 2010;18(3):1879–87.
[47] Guha B, Kyotoku BBC, Lipson M. CMOS-compatible athermal silicon microring resonators. Opt Express 2010;18(4):3487–93.
[48] Guha B, Preston K, Lipson M. Athermal silicon microring electro-optic modulator. Opt Lett 2012;37(12):2253–5.
[49] Manipatruni S, Dokania RK, Schmidt B, Sherwood-Droz N, Poitras CB, Apsel AB, Lipson M. Wide temperature range operation of micrometer-scale silicon electro-optic modulators. Opt Lett 2008;33(19):2185–7.
[50] Li C, Bai R, Shafik A, Tabasy EZ, Tang G, Ma C, Chen C-H, Peng Z, Fiorentino M, Chiang P, Palermo S. A ring-resonator-based silicon photonics transceiver with bias-based wavelength stabilization and adaptive-power-sensitivity receiver. Proc International Solid-State Circuits Conference, San Francisco, 2013.
[51] Cunningham JE, Shubin I, Zheng X, Pinguet T, Mekis A, Luo Y, Thacker H, Li G, Yao J, Raj K, Krishnamoorthy AV. Highly-efficient thermally-tuned resonant optical filters. Opt Express 2010;18(18):19055–63.
[52] Ng H-Y, Wang MR, Li D, Wang X, Martinez J, Panepucci RR, Pathak K. 4×4 wavelength-reconfigurable photonic switch based on thermally tuned microring resonators. Opt Eng 2008;47: Article ID: 044601.
[53] Geng M, Jia L, Zhang L, Yang L, Chen P, Wang T, Liu Y. Four-channel reconfigurable optical add-drop multiplexer based on photonic wire waveguide. Opt Express 2009;17(7):5502–16.
[54] Yu H, Pantouvaki M, Dwivedi S, Verheyen P. Compact thermally tunable silicon racetrack modulators based on an asymmetric waveguide. IEEE Photonic Tech L 2013;25(2):159–62.

[55] Gan F, Barwicz T, Popovic MA, Dahlem MS, Holzwarth CW, Rakich PT, Smith HI, Ippen EP, Kartner FX. Maximizing the thermo-optic tuning range of silicon photonic structures. Proc Photonics in Switching, San Francisco, CA, 2007:67–8.
[56] Watts MR. Adiabatic microring resonators. Opt Lett 2010;35(19):3231–3.
[57] Watts MR, Zortman WA, Trotter DC, Nielson GN, Luck DL, Young RW. Adiabatic resonant microrings (ARMs) with directly integrated thermal microphotonics. Proc Conference on Lasers and Electro-optics, 2009.
[58] DeRose CT, Watts MR, Trotter DC, Luck DL, Nielson GN, Young RW. Silicon microring modulator with integrated heater and temperature sensor for thermal control. Proc Conference on Lasers and Electro-optics, 2010.
[59] Zortman WA, Lentine AL, Trotter DC, Watts MR. Integrated CMOS compatible low power 10Gbps silicon photonic heater-modulator. Proc Optical Fiber Communication Conference, 2012.
[60] Dong P, Qian W, Liang H, Shafiiha R, Feng NN, Feng D, Zheng X, Krishnamoorthy AV, Asghari M. Thermally tunable silicon racetrack resonators with ultralow tuning power. Opt Express 2010;18(19):20298–304.
[61] Dong P, Qian W, Liang H, Shafiiiha R, Feng NN, Feng D, Zheng X, Krishnamoorthy AV, Asghari M. Low power and compact reconfigurable multiplexing devices based on silicon microring resonators. Opt Express 2010;18(10): 9852–8.
[62] Shubin I, Li G, Zheng X, Luo Y, Thacker H, Yao J, Park N, Krishnamoorthy AV, Cunningham JE Integration, processing and performance of low power thermally tunable CMOS-SOI WDM resonators. Opt and Quant Electron 2012;44(12): 589–604.
[63] Chen Y-H, Sun C, Stojanovic V. Scalable electrical-optical thermal simulator for multicores with optical interconnects. Proc IEEE Optical Interconnects, Santa Fe, NM, 2013.
[64] Zheng X, Luo Y, Li G, Shubin I, Thacker H, Yao J, Raj K, Cunningham JE, Krishnamoorthy AV. Enhanced optical bistability from self-heating due to free carrier absorption in substrate removed silicon ring modulators. Opt Express 2012;20(10):11478–86.
[65] Li Q, Ophir N, Xu L, Padmaraju K, Chen L, Lipson M, Bergman K. Experimental characterization of the optical-power upper bound in a silicon microring modulator. Proc IEEE Optical Interconnects Conference, Santa Fe, 2012.
[66] Qiu C, Shu J, Li Z, Zhang X, Xu Q. Wavelength tracking with thermally controlled silicon resonators. Opt Express 2011;19(6):5143–8.
[67] Timurdogan E, Biberman A, Trotter DC, Sun C, Moresco M, Stojanovic V, Watts MR. Automated wavelength recovery for microring resonators. Proc Conference on Lasers and Electro-optics, San Jose, 2012.
[68] Padmaraju K, Logan DF, Zhu X, Ackert JJ, Knights AP, Bergman K. Integrated thermal stabilization of a microring modulator. Opt Express 2013;21(12):14342–50.
[69] Zortman WA, Lentine AL, Trotter DC, Watts MR. Bit error rate monitoring for active wavelength control of silicon microphotonic resonant modulators. IEEE Micro 2013;33(1): 42–52.
[70] Hansch TW, Couillaud B. Laser frequency stabilization by polarization spectroscopy of a reflecting reference cavity. Opt Commun 1980;35(3):441–4.
[71] Cox JA, Trotter DC, Starbuck AL. Integrated control of silicon-photonic micro-resonator wavelength via balanced homodyne locking. Proc IEEE Optical Interconnects Conference, Santa Fe, 2013.
[72] Padmaraju K, Logan DF, Ackert JJ, Knights AP, Bergman K. Microring resonance stabilization using thermal dithering. Proc IEEE Optical Interconnects, Santa Fe, NM, 2013.
[73] Logan DF, Velha P, Sorel M, De La Rue RM, Jessop PE, Knights AP. Monitoring and tuning micro-ring properties using defect-enhanced silicon photodiodes at 1550 nm. IEEE Photonic Tech L 2011;24(4):261–3.
[74] Krishnamoorthy AV, Zheng X, Li G, Yao J, Pinguet T, Mekis A, Thacker H, Shubin I, Luo Y, Raj K, Cunningham JE. Exploiting CMOS manufacturing to reduce tuning requirements for resonant optical devices. IEEE Photonic J 2011;3(3):567–79.